www.whxb.pku.edu.cn

ISSN 1000-6818
CN 11-1892/O6
CODEN WHXUEU

物理化学学报

ACTA PHYSICO-CHIMICA SINICA

第 28 卷 第 1 期 Vol.28 No.1 2012

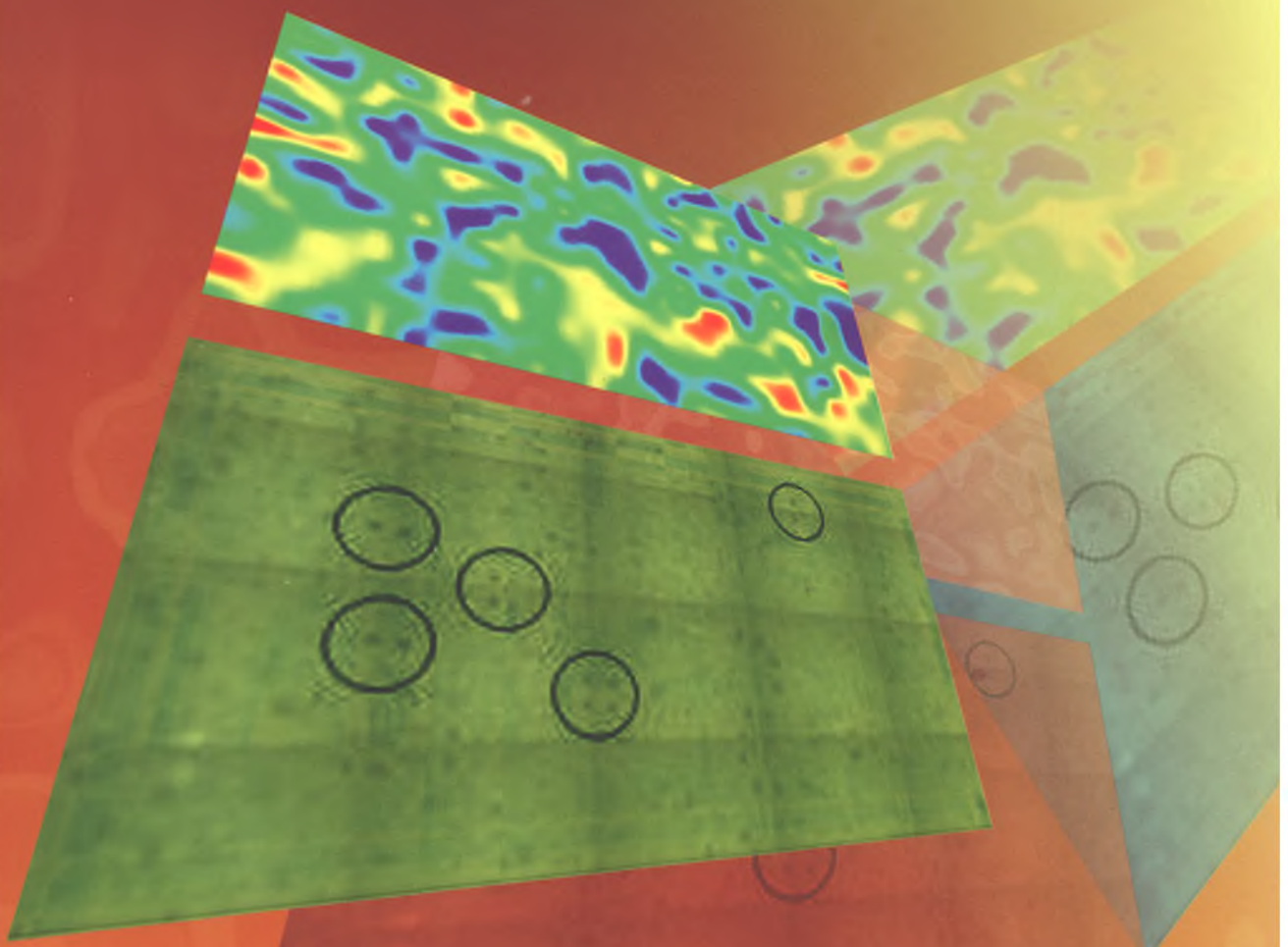

3 2267 3566 4

中国化学会主办
中国科学技术协会主管
北京大学化学学院物理化学学报编辑部出版

物理化学学报(Wuli Huaxue Xuebao)
第 28 卷第 1 期(2012 年 1 月)

目　　次

本期责任编辑: 於秀芝

ACTA PHYSICO-CHIMICA SINICA
Vol. 28 No.1 (January, 2012)

COVER

The cover image presents the IR map and its corresponding optical photo of the micro-arc oxidation (MAO) coating with a cathodic polarization. On page 127, CHANG *et al.* demonstrate that the IR maps and their corresponding optical photos of the MAO coatings with or without a cathodic polarization are much different from each other, and the results show that the cathodic polarization can accelerate the dissolution of $Mg(OH)_2$ and change the structure of the MAO coating.

CONTENTS

REVIEW

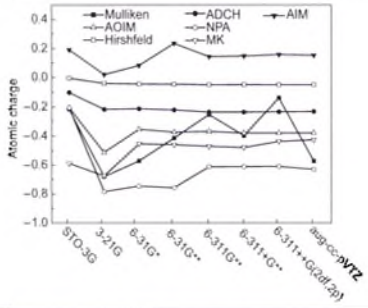

The twelve most commonly used computational methods for the determination of atomic charges are introduced and compared in detail.

THERMODYNAMICS, KINETICS, AND STRUCTURE CHEMISTRY

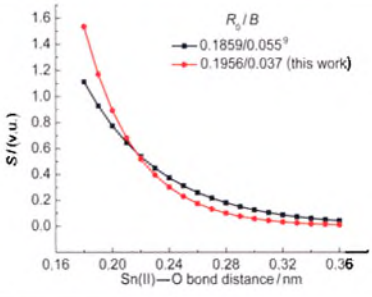

Studies of the bond valence (S) sum can be extremely useful for chemists and crystallographers to analyze the crystal structure of a metal-organic compound or resolve conflict regarding oxidation states.

Kinetic Analysis of a Pyrolysis Process and Hydrogen Generation of Humic Acids of Yimin Lignite Fusain Using the Distributed Activation Energy Model

WANG Chuan-Ge ZENG Fan-Gui
PENG Zhi-Long LI Xia
ZHANG Li

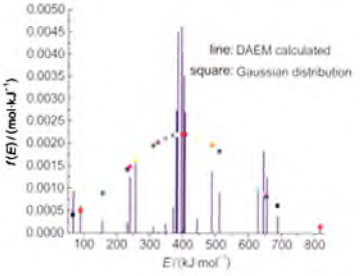

The distribution functions of the activation energy for the pyrolysis and hydrogen generation of the humic acids of fusain (F-HA) and the humic acids of demineralized fusain (DF-HA) exhibit different asymptotic approximations compared to the Gaussian distribution and they appear staged, which indicates that demineralization influences the thermal behavior, the kinetics of pyrolysis, the hydrogen generation of humic acids and, additionally, the reaction mechanism is different in each pyrolitic stage.

Acta Phys. -Chim. Sin. **2012,** *28* (1), 25−36

Thermodynamic Reoptimization of the Fe-P System

CAO Zhan-Min WANG Kun-Peng
QIAO Zhi-Yu DU Guang-Wei

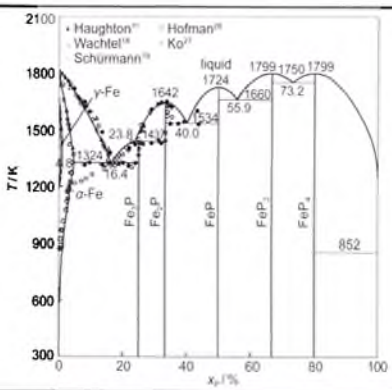

Fe-P is a fundamental binary system of Fe-based, P-containing multicomponent alloys, and is of great importance for the design and processing of advanced materials.

Acta Phys. -Chim. Sin. **2012,** *28* (1), 37−43

THEORETICAL AND COMPUTATIONAL CHEMISTRY

CO Adsorption and Oxidation on Metal-Doped TiO_2 Nanotube Arrays

DONG Hua-Qing PAN Xi
XIE Qin MENG Qiang-Qiang
GAO Jian-Rong WANG Jian-Guo

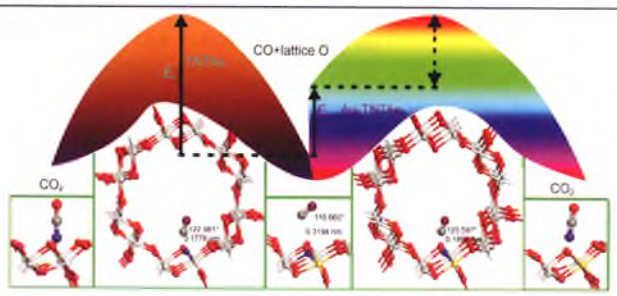

Au- or Pd-doped titania nanotube arrays can significantly enhance CO oxidation compared with the pristine nanotube arrays.

Acta Phys. -Chim. Sin. **2012,** *28* (1), 44−50

Adsorption Properties of CO Molecules on Pt/t-ZrO_2(101) Surfaces

MAN Mei-Ling LU Chun-Hai
CHEN Wen-Kai LI Yi
ZHANG Yong-Fan

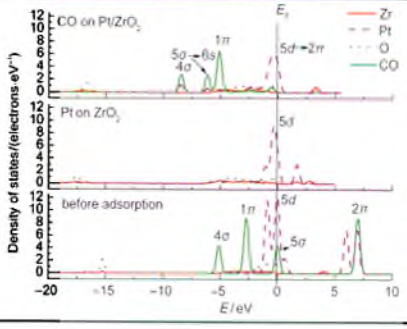

Density of states showed the binding mechanism of CO molecule before and after adsorption onto a Pt/ZrO_2(101) surface. We found that charge transfer was predominantly with π back-donation bonding mechanism of Pt $5d \rightarrow$CO 2π.

Acta Phys. -Chim. Sin. **2012,** *28* (1), 51−57

Microstructure and Jahn-Teller Effect of Cu-Zn-Mg-Al Layered Double Hydroxides

WANG Li-Geng SHI Wei
YAO Ping NI Zhe-Ming
LI Yuan LIU Jiao

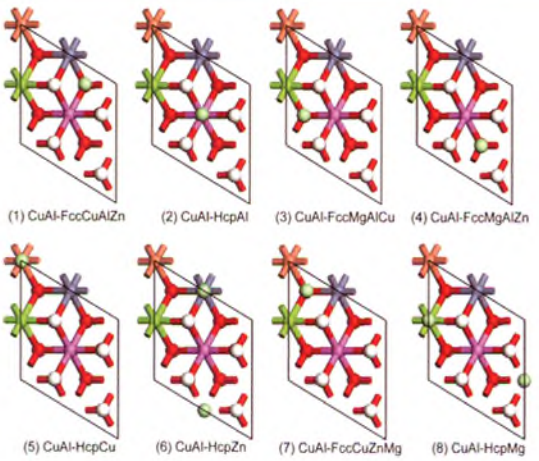

Acta Phys. -Chim. Sin. **2012,** *28* (1), 58−64

Research was undertaken into the microstructure and the Jahn-Teller effect of the Cu-Zn-Mg-Al layered double hydroxides.

Resonance Raman Spectroscopy and Density Functional Theory Investigations on the Excited State Structural Dynamics of *N*-Methylpyrrole-2-carboxaldehyde and Its Solvent Effect

XU Zong-Ping ZHAO Yan-Ying
WANG Hui-Gang ZHENG Xu-Ming

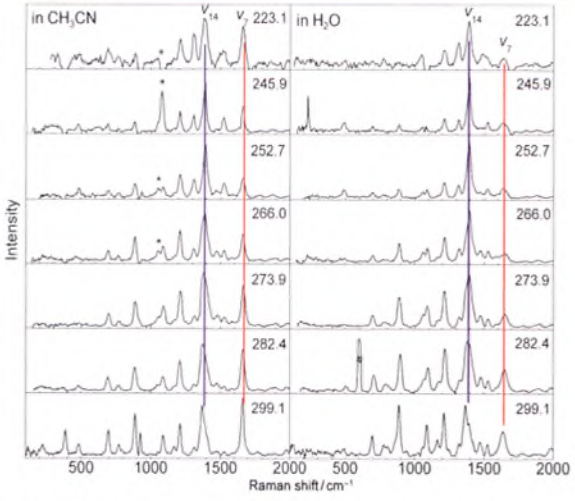

The relative intensity of the C=O stretch mode ν_7 *versus* the C6−N1−C2/C2−C3−C4 anti-symmetry stretch mode ν_{14} is solvent dependent and laser excitation wavelength dependent. The intensity change in the C=O stretch mode ν_7 indicates a change in the displacement of the C=O mode for excited state changes and correlates with the S_1/S_2 state-mixing or curve-crossing in the Franck-Condon region.

Acta Phys. -Chim. Sin. **2012,** *28* (1), 65−72

One-Electron Redox Characteristics of One-Hydroxyl Radical Adducts of A-T Base Pairs

HOU Ruo-Bing SUN Yan-Li
WANG Bei-Bei

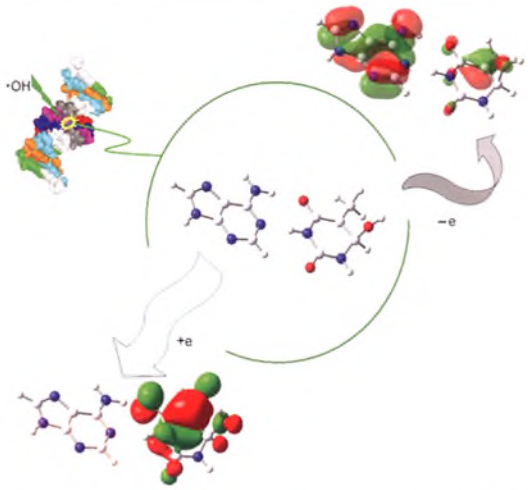

Acta Phys. -Chim. Sin. **2012,** *28* (1), 73−77

One-electron capture reaction is an important redox feature of one-hydroxyl radical adducts of adenine-thymine (A-T) base pairs.

Comparison of D-SS and D-ST Dyes as Photo Sensitizers in Dye-Sensitized Solar Cells

ZHAN Wei-Shen PAN Shi
WANG Qiao LI Hong
ZHANG Yi

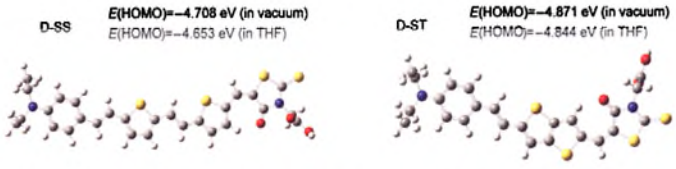

Acta Phys. -Chim. Sin. **2012,** *28* (1), 78−84

The HOMO energy level of D-SS is higher than the redox energy level of the electrolyte, so excited D-SS molecules cannot be recovered by accepting an electron from the electrolyte.

ELECTROCHEMISTRY AND NEW ENERGY

Effect of Intermittent Microwave Heating on the Performance of Catalysts for Oxygen Reduction Reaction

YIN Shi-Bin LUO Lin
JING Sheng-Yu ZHU Qiang-Qiang
QIANG Ying-Huai

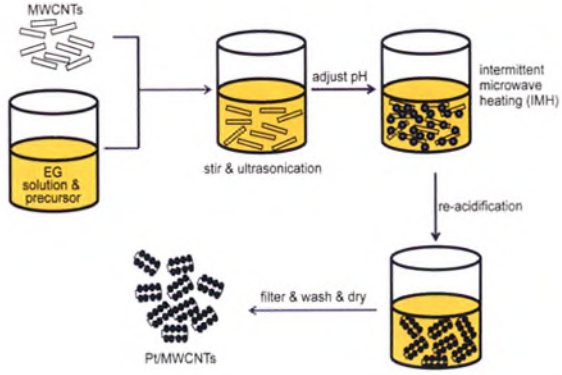

Acta Phys. -Chim. Sin. **2012,** *28* (1), 85−89

Intermittent microwave heating method is an economical, controllable, and scalable method to allow the mass production of nanomaterials.

Discharge Performance of Alkaline Sulfide Fuel Cells Using Non-Precious Anode Catalysts

FAN Yu-Qian SHAO Hai-Bo
WANG Jian-Ming LIU Liang
ZHANG Jian-Qing CAO Chu-Nan

Acta Phys. -Chim. Sin. **2012,** *28* (1), 90−94

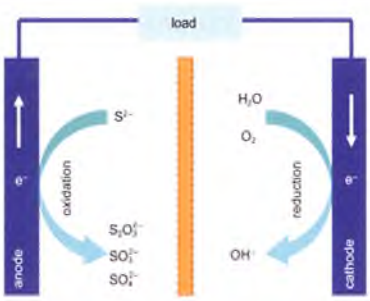

We demonstrate that alkaline sulfide fuel cells containing non-precious carbon-based catalysts can exhibit a considerable power output, while sulfides are deeply oxidized.

Preparation, Structure and Properties of $Pr_{1.2}Sr_{0.8}NiO_4$ Cathode Materials for Intermediate-Temperature Solid Oxide Fuel Cells

YANG Jun-Fang CHENG Ji-Gui
FAN Yu-Meng WANG Rui
GAO Jian-Feng

Acta Phys. -Chim. Sin. **2012,** *28* (1), 95−99

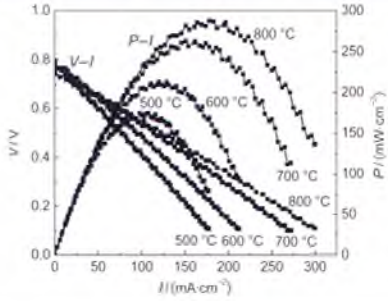

$Pr_{1.2}Sr_{0.8}NiO_4$ (PSNO) material with a K_2NiF_4-type structure was prepared by the glycine-nitrate process. The material shows good electrochemical and thermal properties. It is a potential cathode material for use in intermediate-temperature solid oxide fuel cells.

Electrochemical Performance of Vanadium Modified $LiFe_{0.5}Mn_{0.5}PO_4$/C Cathode Materials for Lithium-Ion Batteries

GONG Qiang WANG Hong
LIAO Xiao-Zhen MA Wei
HE Yu-Shi MA Zi-Feng

Acta Phys. -Chim. Sin. **2012,** *28* (1), 100−104

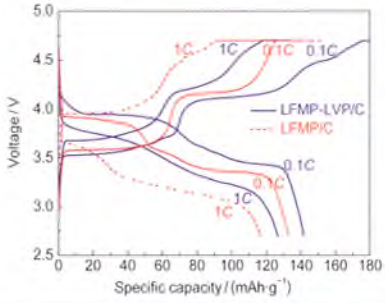

Vanadium modification can be an effective method to improve the electrochemical performance of olivine-type cathode materials.

Synthesis and Electrochemical Performance of Graphene Modified $LiFePO_4$ Cathode Materials

XU Ke SHEN Lai-Fa
MI Chang-Huan ZHANG Xiao-Gang

Acta Phys. -Chim. Sin. **2012,** *28* (1), 105−110

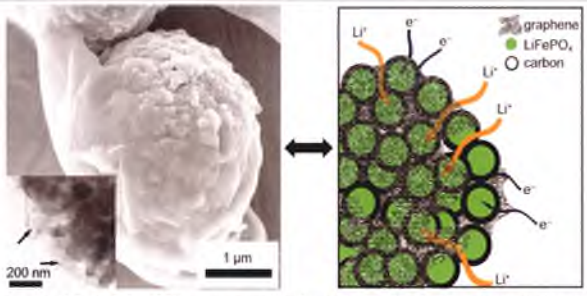

Graphene modified $LiFePO_4$ was synthesized by a hydrothermal method and shown to possess excellent electrochemical properties.

Preparation of Ni and Ni-Al Alloys from $2AlCl_3/Et_3NHCl$ Ionic Liquid by Electrodeposition

GAO Li-Xia WANG Li-Na
QI Tao YU Jiang

Acta Phys. -Chim. Sin. **2012,** *28* (1), 111−120

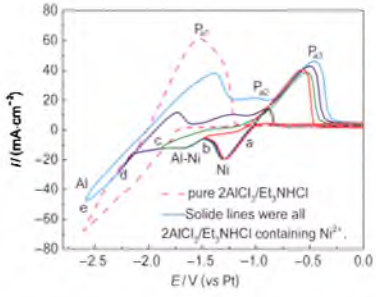

The mechanism and the influence of experimental conditions on the composition and surface morphology of Ni-Al alloy electrodeposition on Cu electrodes from $2AlCl_3/Et_3NHCl$ ionic liquids were investigated.

Corrosion Behavior of Tinplates in a Functional Beverage

XIA Da-Hai SONG Shi-Zhe
WANG Ji-Hui BI Hui-Chao
HAN Zhe-Wen

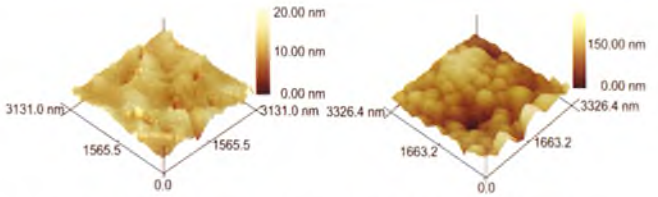

We investigated the corrosion mechanism of a tinplate in a functional beverage and found that the tinplate was mainly corroded by the organic acids that exist in the functional beverage.

Acta Phys. -Chim. Sin. **2012,** *28* (1), 121-126

Polarization Behavior of Magnesium Alloy AZ91D with Micro-Arc Oxidation Coating in NaCl Solution

CHANG Lin-Rong CAO Fa-He
CAI Jing-Shun LIU Wen-Juan
ZHENG Jun-Jun ZHANG Jian-Qing
CAO Chu-Nan

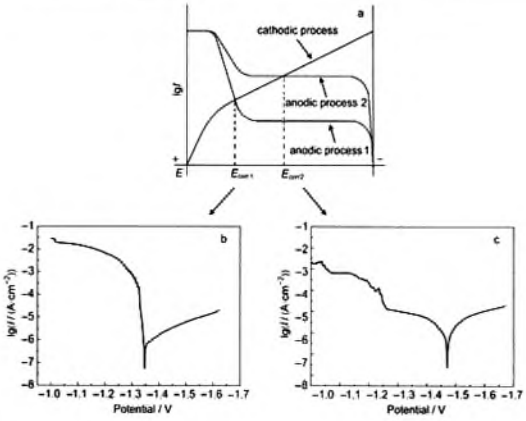

The polarization curve of a micro-arc oxidation (MAO) coating depends on both its main composition and microstructure because of its instability in NaCl solution.

Acta Phys. -Chim. Sin. **2012,** *28* (1), 127-136

Adsorption Mechanism of Nicotinic Acid onto a Passive Iron Surface

TIAN Hui-Wen LI Wei-Hua
WANG Da-Peng HOU Bao-Rong

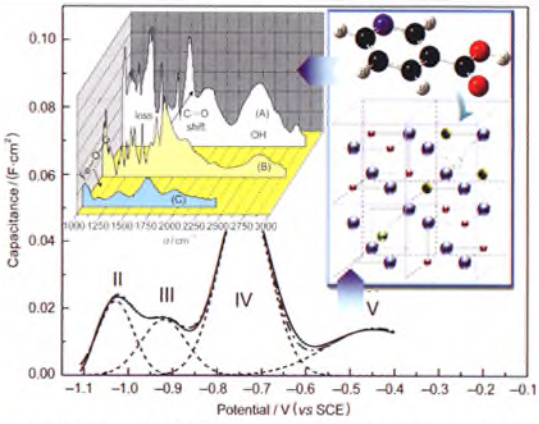

Adsorption mechanism of nicotinic acid onto passive iron is attributed to its ability to form a surface complex.

Acta Phys. -Chim. Sin. **2012,** *28* (1), 137-145

SOFT MATTER

Application of Anion-Cation Pair Surfactant Systems to Achieve Ultra-Low Oil-Water Interfacial Tension

HAN Xia CHENG Xin-Hao
WANG Jiang HUANG Jian-Bin

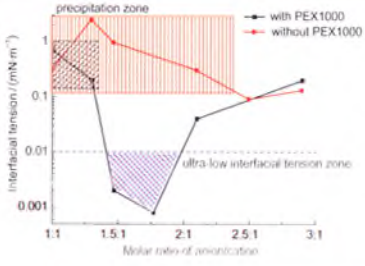

Ultra-low interfacial tension was achieved in realistic mixed systems combining ion pairs and non-ionic agents.

Acta Phys. -Chim. Sin. **2012,** *28* (1), 146-153

Preparation of a Ag@AgCl-Modified $TiO_{2-x}C_x$ Photocatalyst and Its Performance for Degradation of Pollutants under Visible Light

NIE Long-Hui HU Yao
ZHANG Wang-Xi

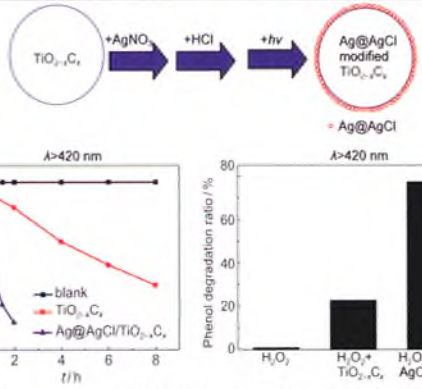

The photocatalytic activity of $TiO_{2-x}C_x$ under visible light for the degradation of methyl orange and phenol was greatly improved after modification with Ag@AgCl.

Acta Phys. -Chim. Sin. **2012,** *28* (1), 154−160

Preparation and Properties of N-F Co-Doped TiO_2 Photocatalyst with Wide Range Light Response and Multipore Structure from Ionic Liquid-Water Mixture Solvent

CHEN Xiao-Yun LU Dong-Fang
HUANG Jin-Feng LU Yan-Feng
ZHENG Jian-Qiang

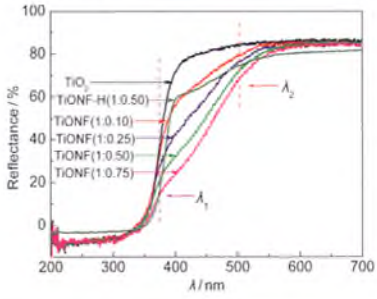

TiONF synthesized in an ionic liquid-water mixture solvent exhibited high activity under UV, Vis, and solar light irradiation.

Acta Phys. -Chim. Sin. **2012,** *28* (1), 161−169

Preparation of CuO-ZnO-ZrO_2 by Citric Acid Combustion Method and Its Catalytic Property for Methanol Synthesis from CO_2 Hydrogenation

GUO Xiao-Ming MAO Dong-Sen
LU Guan-Zhong WANG Song

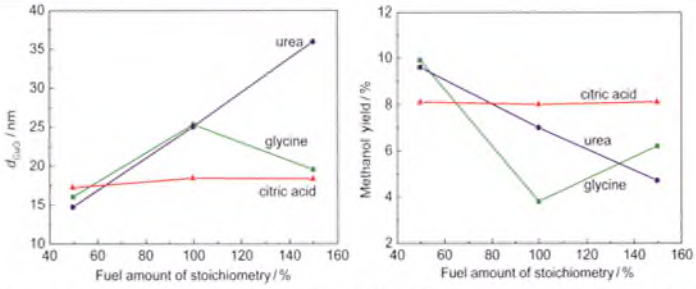

Trends of the properties of CuO-ZnO-ZrO_2 prepared by combustion method with the quantity of fuel are different when various fuel types are used.

Acta Phys. -Chim. Sin. **2012,** *28* (1), 170−176

Hydrogenation of Glucose Using Ru/Activated Carbon Catalysts: Effects of Modification Methods on Surface Properties of Activated Carbon

XU San-Kui LI Li-Min
GUO Nan-Nan SU Yun-Lai
ZHANG Peng

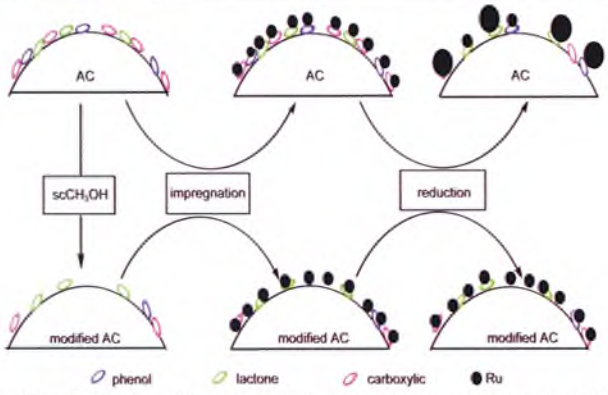

$scCH_3OH$ modification reduces the amount of surface unstability groups of carbon, can increase the dispersion of Ru and the activity.

Acta Phys. -Chim. Sin. **2012,** *28* (1), 177−183

Effect of Surface Structure of α-Fe_2O_3 on the Selective Catalytic Reduction of NO by NH_3

YANG Xing-Ye LI Bin
SUN Liang HUANG Zhi-Wei
CHENG Xiao-Min ZHANG Tao-Wei
TANG Xing-Fu

Acta Phys. -Chim. Sin. **2012,** *28* (1), 184-188

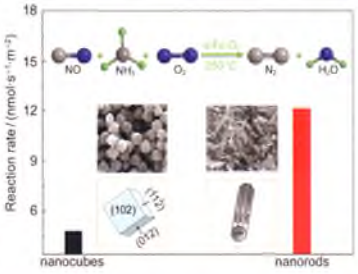

α-Fe_2O_3 nanorods with exposed {110} faces with a high density of Fe atoms show higher activity for the selective catalytic reduction of NO with NH_3 than nanocubes with exposed {012} faces.

Influence of Functional Group Decoration on Gas Adsorption in MOF-5

CHEN Chi PANG Jun
HAN Shuang ZHANG Bi-Xia
HUANG Yuan MIAO Ling
JIANG Jian-Jun

Acta Phys. -Chim. Sin. **2012,** *28* (1), 189-194

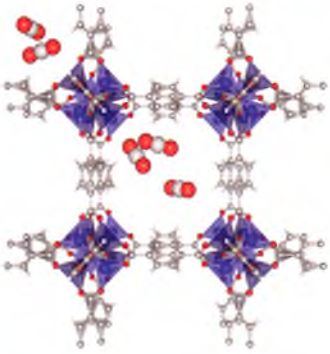

The adsorption of CO_2 mixture gases in the decorated MOF-5 with different functional groups ($-NO_2$, $-NH_2$, $-CH_3$, $-OZn$) was studied based on the tight binding approximation method. $-NO_2$ decorated MOF-5 shows an obvious selective adsorption ability for different gases in air (O_2, N_2, H_2O, CO_2) and for industrial waste gases (CO_2, CO, NO, NO_2, SO_2, SO_3).

Grafting Morphologies of TEPA on SBA-15(P) and Its Effect on CO_2 Adsorption Performance

YANG Yong-Hong LI Fen-Fen
YANG Cheng ZHANG Wen-Yu
WU Jin-Hu

Acta Phys. -Chim. Sin. **2012,** *28* (1), 195-200

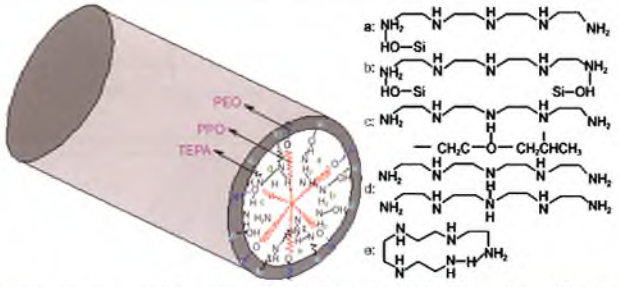

A dynamic impregnated process effectively avoided the formation of hydrogen bond between intra-molecules and inter-molecules.

Effect of Primary Alkylamine Adsorption on Muscovite Hydrophobicity

LIU Zhen LIU Gou-Sheng
YU Jian-Guo

Acta Phys. -Chim. Sin. **2012,** *28* (1), 201-207

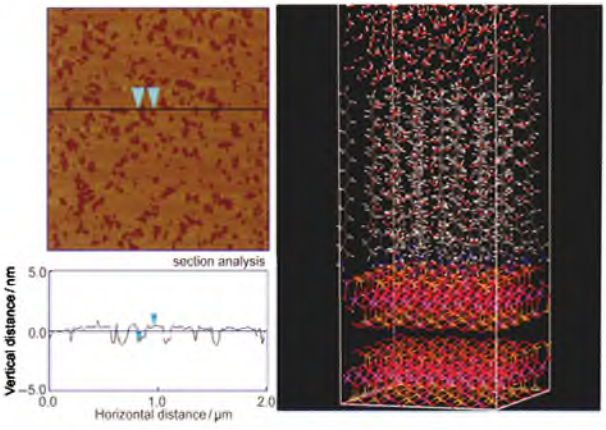

Muscovite hydrophobicity was enhanced by the adsorption of alkylamine. Longer alkyls gave better results.

Synthesis of CdS Quantum Dots and Their Optical Limiting Effect

ZHENG Li-Si FENG Miao
ZHAN Hong-Bing

Acta Phys. -Chim. Sin. **2012,** *28* (1), 208-212

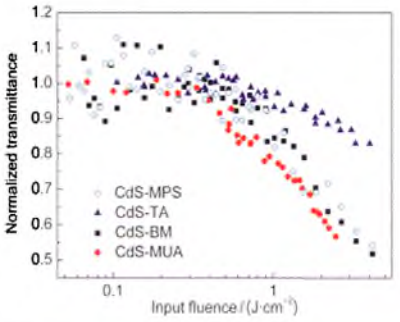

Four kinds of CdS QDs with different organic capping agents, namely, (3-mercaptopropyl) trimethoxysilane (MPS), thioglycolic acid (TA), benzyl mercaptan (BM), and 11-mercaptoundecanoic (MUA) were synthesized. Their nonlinear behaviors differed because of differences in the size, surface morphology, and defect concentration of the synthesized QDs.

Laser Flash Photolysis Study on Electron Transfer Oxidation Reaction of Tryptophan or Tyrosine with Triplet State Vitamin K_3

TANG Rui-Zhi LI Hai-Xia
LIU Yan-Cheng ZHANG Peng
CAO Xi-Yan WANG Wen-Feng

Acta Phys. -Chim. Sin. **2012,** *28* (1), 213-216

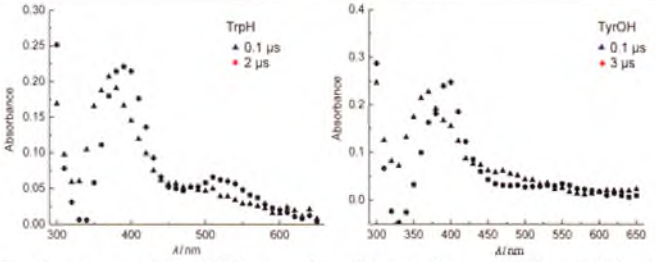

The electron transfer oxidation reaction of tryptophan or tyrosine with the triplet state of vitamin K_3 was investigated in acetonitrile/water solution.

Investigation on Photocurrent Polarity of a Bulk Heterojunction Organic Photovoltaic Device Using a Ferroelectric Thin Film

LI Bo

Acta Phys. -Chim. Sin. **2012,** *28* (1), 217-222

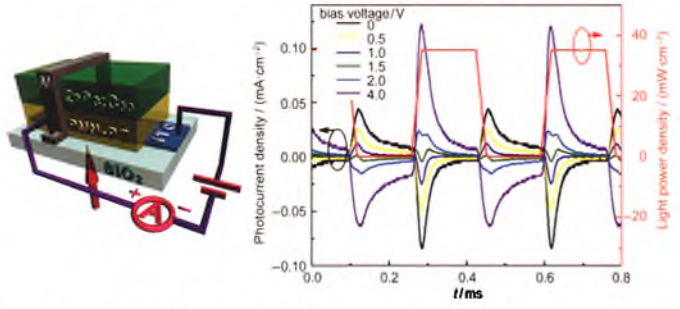

The photocurrent polarity of a bulk heterojunction organic photovoltaic device was investigated and controlled using a ferroelectric thin film.

Structure and Florescence Emission Properties of a Polymer-Rare Earth Complex Composed of Aryl Carboxylic Acid-Functionalized Polysulfone and Tb(III)

ZHANG Rui-Xia GAO Bao-Jiao
WEI Xiao-Peng

Acta Phys. -Chim. Sin. **2012,** *28* (1), 223-231

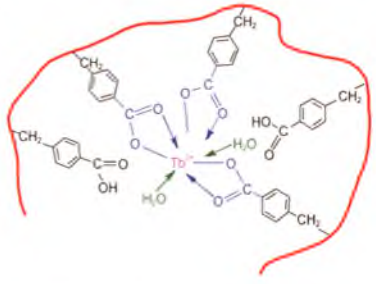

The polymer-rare earth complex PSF-$(BA)_5$-Tb(III)-$(Phen)_1$ exhibits the very strong characteristic fluorescence emissions of Tb(III) and has excellent thermal stability.

Effects of CdSe Layer Number on the Optical Properties and Microstructures of CdTe/CdSe (II) Core/Shell Quantum Dots

PENG Jing FANG Xiao-Ming
CHEN Zhi-Hong ZHANG Zheng-Guo

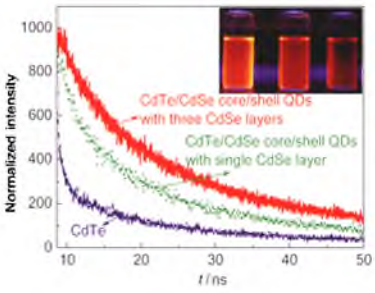

The optical properties of CdTe/CdSe (II) core/shell quantum dots (QDs) can be tuned by changing the number of CdSe layers. As the number of CdSe layers is increased, the optical absorption spectra of the CdTe/CdSe core/shell QDs cover a wider range and extend to longer wavelengths, the intensity of fluorescence emission gradually decreases, and the fluorescence lifetime increases significantly.

Acta Phys. -Chim. Sin. **2012,** *28* (1), 232−238

Fabrication of a Self-Healing Pure SiC Coating by a Two-Step Technique

CHEN Yang WANG Cheng-Guo
ZHAO Wei

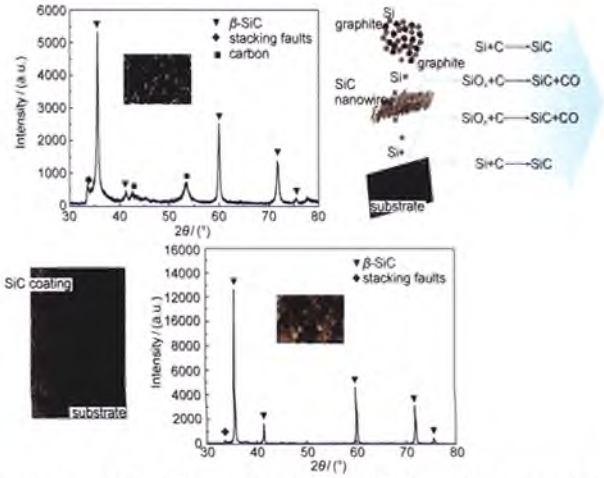

Self-healing pure SiC coating was fabricated and it showed an improved oxidation resistance in C/C composites.

Acta Phys. -Chim. Sin. **2012,** *28* (1), 239−244

Influence of Reductive Treatment on the Performance of CeO_2-ZrO_2-Al_2O_3 Composite Oxide

XIAO Yi-Hong YANG Huang-Gen
CAI Guo-Hui ZHENG Yong
ZHENG Ying WEI Ke-Mei

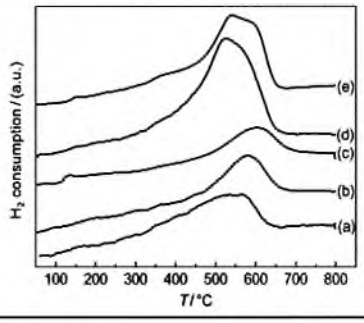

A $CeAlO_3$ phase was formed after CZA was reductively treated at 950 °C and an increase in temperature benefited the formation of $CeAlO_3$. The oxygen storage capacity and reducibility of the material were remarkably influenced by the formation of a $CeAlO_3$ phase after CZA was reductively aged.

Acta Phys. -Chim. Sin. **2012,** *28* (1), 245−250

Growth Mechanism and Morphology of ZnO/eosin-Y Hybrid Thin Films

MARÍ Bernabé SINGH Krishan-Chander
MOLLAR Miguel MOYA Mónica
RANA Ravi

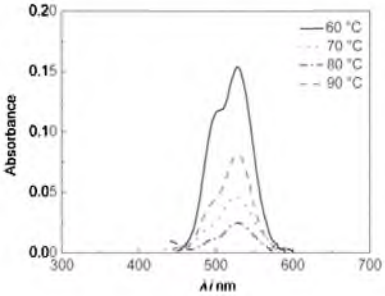

Thin hybrid films of ZnO/eosin-Y were fabricated in aqueous and non-aqueous baths containing a dye. Films prepared in a non-aqueous bath were non-porous and did not adsorb dye, while those grown in aqueous media were porous and adsorbed dye during the deposition of ZnO, reaching the maximum dye adsorption when ZnO was deposited at 60−70 °C.

Acta Phys. -Chim. Sin. **2012,** *28* (1), 251−256

Effects of CdSe Layer Number on the Optical Properties and Microstructures of CdTe/CdSe (II) Core/Shell Quantum Dots

PENG Jing FANG Xiao-Ming
CHEN Zhi-Hong ZHANG Zheng-Guo

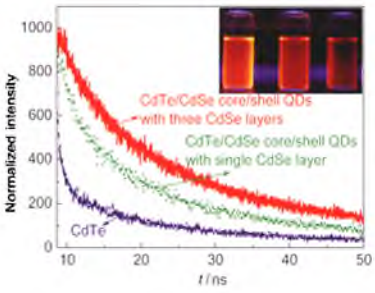

The optical properties of CdTe/CdSe (II) core/shell quantum dots (QDs) can be tuned by changing the number of CdSe layers. As the number of CdSe layers is increased, the optical absorption spectra of the CdTe/CdSe core/shell QDs cover a wider range and extend to longer wavelengths, the intensity of fluorescence emission gradually decreases, and the fluorescence lifetime increases significantly.

Acta Phys. -Chim. Sin. **2012,** *28* (1), 232−238

Fabrication of a Self-Healing Pure SiC Coating by a Two-Step Technique

CHEN Yang WANG Cheng-Guo
ZHAO Wei

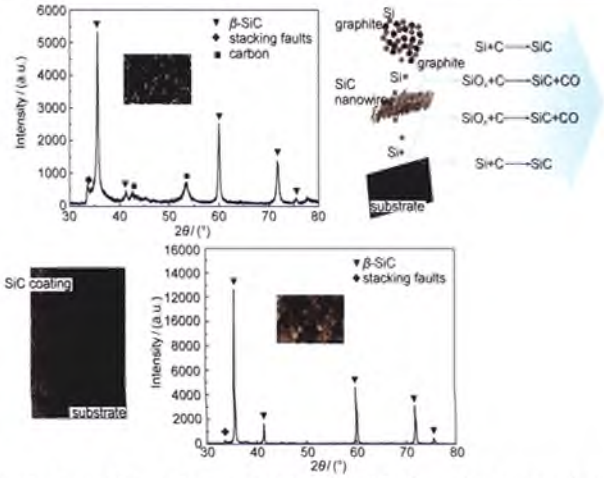

Self-healing pure SiC coating was fabricated and it showed an improved oxidation resistance in C/C composites.

Acta Phys. -Chim. Sin. **2012,** *28* (1), 239−244

Influence of Reductive Treatment on the Performance of CeO_2-ZrO_2-Al_2O_3 Composite Oxide

XIAO Yi-Hong YANG Huang-Gen
CAI Guo-Hui ZHENG Yong
ZHENG Ying WEI Ke-Mei

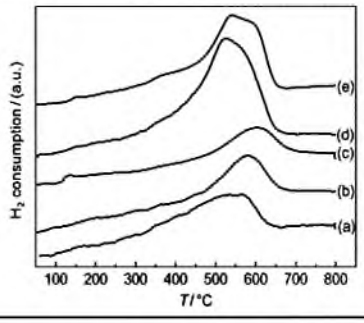

A $CeAlO_3$ phase was formed after CZA was reductively treated at 950 °C and an increase in temperature benefited the formation of $CeAlO_3$. The oxygen storage capacity and reducibility of the material were remarkably influenced by the formation of a $CeAlO_3$ phase after CZA was reductively aged.

Acta Phys. -Chim. Sin. **2012,** *28* (1), 245−250

Growth Mechanism and Morphology of ZnO/eosin-Y Hybrid Thin Films

MARÍ Bernabé SINGH Krishan-Chander
MOLLAR Miguel MOYA Mónica
RANA Ravi

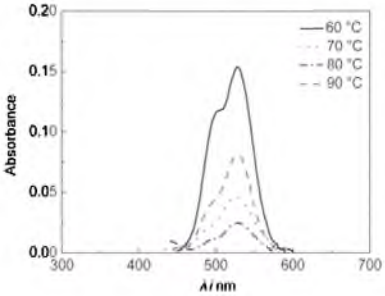

Thin hybrid films of ZnO/eosin-Y were fabricated in aqueous and non-aqueous baths containing a dye. Films prepared in a non-aqueous bath were non-porous and did not adsorb dye, while those grown in aqueous media were porous and adsorbed dye during the deposition of ZnO, reaching the maximum dye adsorption when ZnO was deposited at 60−70 °C.

Acta Phys. -Chim. Sin. **2012,** *28* (1), 251−256